[24] A. Karma. Spiral breakup in model equations of action potential propagation in cardiac tissue. *Physical Review Letters*, 71(7):1103–1106, 1993.

[12] B.Y. Kogan, W.J. Karplus, B.S. Billett, and W.G. Stevenson. Excitation wave propagation within narrow pathways: Configurations facilitating unidirectional block and reentry. *Physica D*, 59:275–296, 1992.

[13] P.I. Nadapurkar and A.T. Winfree. A computation study of twisted linked scroll waves in excitable media. *Physica D*, 29:69–83, 1987.

[14] J.M. Davidenko, A.V. Pertsov, R. Salomonsz, W. Baxter, and J. Jalife. Stationary and drifting spiral waves of excitation in isolated cardiac muscle. *Nature*, 355:349–351, January 1992.

[15] Arkady M. Pertsov, Jorge M. Davidenko, Remy Salomonsz, William T. Baxter, and Jose Jalife. Spiral waves of excitation underlie reentrant activity in isolated cardiac muscle. *Circ. Res.*, 72(3):631–650, 1993.

[16] Frans J. L. van Capelle and M.A. Alessie. Computer simulation of anisotropic impulse propagation: Characteristics of action potentials during re-entrant arrythmias. In A. Goldbeter, editor, *Cell to Cell Signalling: From Experiments to Theoretical Models.*, pages 577–587, 1989.

[17] Frans J. L. van Capelle. Propagation and reentry in two dimentions. In Douglas P. Zipes and Jos Jalife, editors, *Cardiac electrophysiology : from cell to bedside*, pages 175–182, 1990.

[18] Mayer Landau, Paco Lorente, Jacques Henry, and Stephane Canu. Hysteresis phenomena between periodic and stationary solutions in a model of pacemaker and nonpacemaker coupled cardiac cells. *J. Math. Biol.*, 25:491–509, 1987.

[19] A.V. Panfilov and A.V. Holden. Computer simulation of re-entry sources in myocardium in two and tree dimensions. *J. theor Biol.*, 161:271–285, 1993.

[20] S. Weidmann. Electrical constants of trabecular muscle from mammalian heart. *J. Physiol.*, 210:1041–1054, 1970.

[21] R.E. Ten Eick, C.M. Baumgarten, and Singer D.H. Ventricular dysrithmia. In E.H. Sonnenblick and M. Lesch, editors, *Sudden Cardiac Death*, pages 73–104, New York, 1981.

[22] B. Victorri, A. Vinet, F.A. Roberge, and J.-P. Drouhard. Numerical integration in the reconstruction of cardiac action potentials using Hodgkin-Huxley type models. *Computers and Biomedical Research*, 18:10–23, 1985.

[23] Peng S. Chen and Hrayr S. Karagueuzian. Personal communication, 1993.

REFERENCES

[1] G.W. Beeler and H. Reuter. Reconstruction of the action potential of ventricular myocardial fibers. *J. Physiol.*, 268, 1977.

[2] L. Ebihara and E.A. Johnson. Fast sodium current in cardiac muscle: A quantitative description. *Biophys. J.*, 32:779–790, 1980.

[3] C. Luo and Y. Rudy. A model of the ventricular cardiac action potential. *Circ. Res.*, 68:1501–1526, 1991.

[4] Andrew E. Pollard, Mary Jo Burgess, and Kenneth W. Spitzer. Computer simulations of three-dimensional propagation in ventricular myocardium. effects of intramural fiber rotation and inhomogeneous conductivity on epicardial activation. *Circ. Res.*, 72(4):744–756, 1993.

[5] B.J. Roth. Action potential propagation in a thick strand of cardiac muscle. *Circul. Res.*, 68:162–173, 1991.

[6] F.B. Gulko and A.A. Petrov. Mechanism of the formation of closed pathways of conduction in excitable media. *Biofizika*, 17:271–282, 1972.

[7] R. FitzHugh. Mathmatical models of excitation and propagation in nerve. In H.P. Schwan, editor, *Biological Engineering*, chapter 1, pages 1–85. McGraw-Hill, New York, 1969.

[8] Frans J. L. van Capelle and Dirk Durrer. Computer simulation of arrythmias in a network of coupled excitable elements. *Circ. Res.*, 47(3):454–466, 1980.

[9] A.M. Pertsov, R.N. Chramov, and A.V. Panfilov. Sharp increase in refractory period induced by oxidation suppression in FitzHugh-Nagumo model. New mechanism of anti-arrhythmic drug action. *Biofizika*, 6, 1981. (in Russian).

[10] V.S. Zykov. The kinematics of spiral wave nonstationary circulation in excitable media. *Biofizika*, 32:337–340, 1987.

[11] B.Y. Kogan, W.J. Karplus, B.S. Billett, A.T. Pang, H.S. Karagueuzian, and Khan S.S. The simplified FitzHugh-Nagumo model with action potential duration restitution: Effects on 2-d wave propagation. *Physica D*, 50:327–340, 1991.

Fig. 9 illustrates the AP obtained after adjusting the model to the APD data from physiological experiments with the injection of cromakalim [23]. The principle characteristics of this AP are: $APD = 112\ msec$, $\dot{V}_{max} = 398\ V/sec$, $|V_{max}| = 95.3\ mV$. These characteristics are obtained for the following values of model parameters: $C = 1\ \mu F/cm^2$, $\bar{T} = 0.22$, $f^* = 4f$ with the others maintained at their original values. The difference in shape between these APs can be eliminated by adjusting parameters of the model as it is shown above, when more precise experimental data will be available.

CONCLUSIONS

1. The original version of the VC-D model with the original values of the parameters permits the simulation of heart muscle tissue for the special case characterized by low maximal rate of depolarization process and low velocity of propagation.

2. Using the VC-D model it is possible to attain the desired rate of depolarization by decreasing the membrane capacitance from 10 $\mu F/cm^2$ to 1 $\mu F/cm^2$ and by increasing the amplitude of the function $f(V)$.

3. The required APD can be adjusted by changing the amplitude of the function $i_1(V)$. The greater the amplitude of $i_1(V)$, the smaller becomes the APD. The same effect can be achieved by changing the value of the time constant $\bar{T}$. The greater $\bar{T}$, the longer is the APD.

4. To attain the required experimental curve of APD restitution in the VC-D model one can use the method proposed in [11] for the FitzHugh - Nagumo model.

5. As shown above, the effect of variable Y growth on the rate of the depolarization process is reduced with the increase of the amplitude of the function $f(V)$ and can be completely avoided.

ACKNOWLEDGMENT

Research in the use of massive parallelism for system simulation in the UCLA Computer Science Department is supported in part by the NASA/Dryden Research Center under Grant NCC 2–374 and NSF Grant BBS 87–14206.

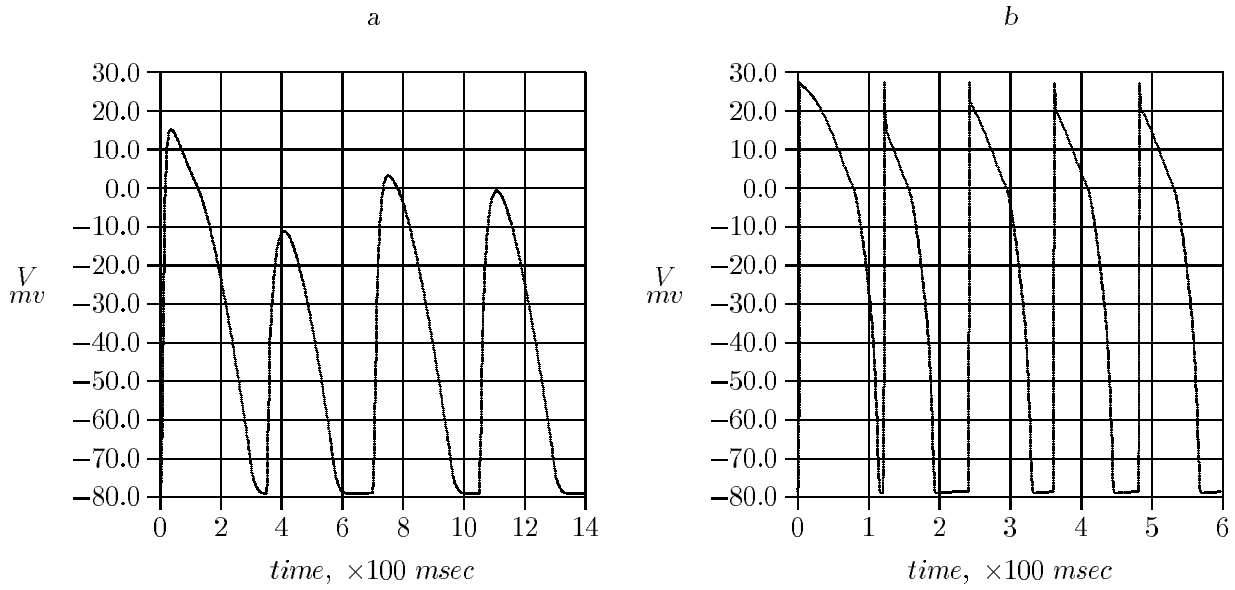

FIG. 8. The action potentials produced by the repeatable excitation for the modified VC-D model without (a) and with (b) the introduction of the Y^*.

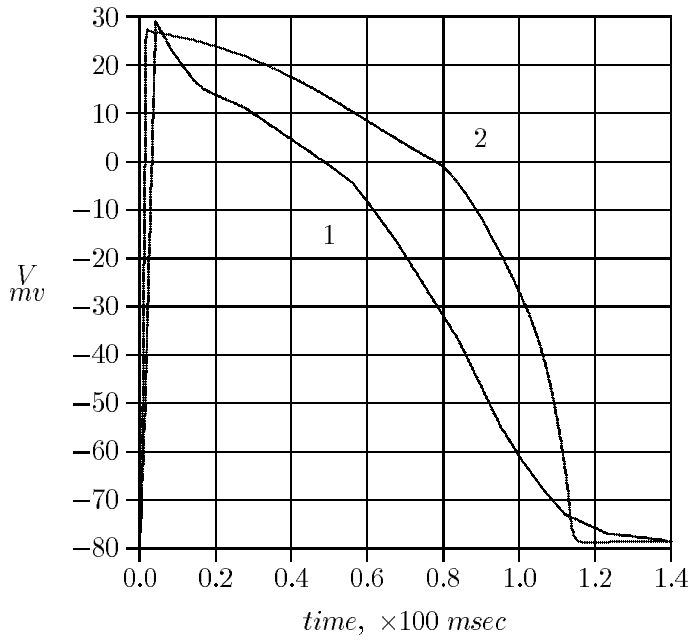

FIG. 9. The AP obtained after adjusting the model to match the data of physiological experiments with the injection of cromakalim. 1 - experimental data, 2 - simulation.

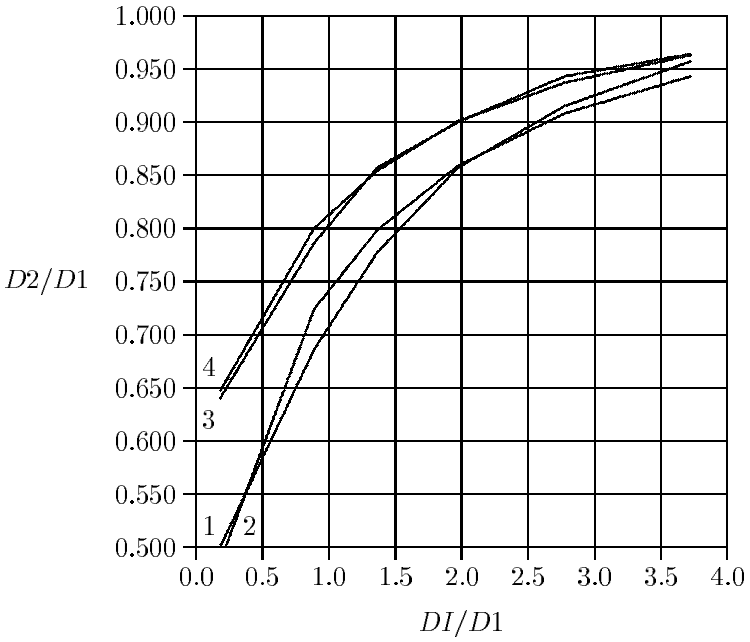

FIG. 7. Comparison of the APD restitution curve experimental data (1,3) to simulate results (2,4). (1,2) - normal heart, (3,4) - ischemic heart.

function of Y and $\dot{Y}$ as:

$$T = \begin{cases} 0.5 & \text{if } \frac{\partial Y}{\partial t} > 0 \\ 0.5K_1 & \text{if } \frac{\partial Y}{\partial t} < 0,\ Y \geq Y_{lim} \\ 0.5K_2 & \text{otherwise} \end{cases} \tag{19}$$

The coefficient K_2 can be found directly from the given restitution curve and K_1 and Y_{lim} in the process of final adjustment. For example, for restitution curves "1" and "2" presented in Fig. 3 we obtain $K_1 = 0.2,\ Y_{lim} = 0.90,\ K_2 = 8.0$ and $K_1 = 0.2,\ Y_{lim} = 0.78,\ K_2 = 7.0$ respectively. The computer simulation results obtained using these fitting parameters are presented in Fig. 7 with the experimental APD restitution curves [21]. The comparison shows the accuracy of the fitting process to be adequate. The repeated stimulation with APD restitution corresponding to an ischemic heart (curve 3 in Fig. 7) shows the well expressed alternance in APD (see Fig. 8a). Note, that the duration of the periodic AP after transient period came to a steady state value smaller than the duration of the first AP. The amplitudes of the AP in the successive cycles are the same (see Fig. 8b), but the AP rapidly decays down after reaching the repolarization peak. This phenomenon is the result of the introduction of Y^* in (6).

MODIFICATION OF THE VAN CAPELLE AND DURRER MODEL

The VC-D model allows to be modified to fit the experimental data which reflect the major global characteristics of AP (APD, APD restitution, amplitude of AP, maximum speed of depolarization, shape of AP, relaxation coefficient).

The slow rate of depolarization inherent in the original version [8] can be increased by decreasing the cell membrane capacity from 10 $\mu F/cm^2$ to 1 $\mu F/cm^2$ (from $\bar{C} = 0.1$ to $\bar{C} = 0.01$). The computations show that in this case the characteristics of AP are: $\dot{V}_{max} = 74\ mV/msec$, $APD = 165\ msec$, $|V_{max}| = 88.3\ mV$, $\rho = 120$. A further increase of depolarization rate can be achieved by increasing $f(V)$ in (6). Designating $f^*(V) = Kf(V)$, and letting $K > 1$ leads to an increase of $\dot{V}_{max}$, while $K < 1$ leads to a decrease. For example, when $K = 4$ we obtain: $\dot{V}_{max} = 269\ mV/msec$, $APD = 234\ msec$, $|V_{max}| = 95.0\ mV$, $\rho = 664$. The increase of depolarization rate is accompanied by an increase of APD.

In the original VC-D model, the gate variable Y affects not only the repolarization but also the depolarization phases of AP. This leads to a decrease of the depolarization rate and the appearance of an unnatural dependence of the amplitude of repeatable AP on Y. To minimize the effect of Y growth during the depolarization phase of AP, we propose to introduce the new variable Y^* in (6) instead of Y, so that

$$Y^* = \begin{cases} 0 & \text{if } \frac{\partial V}{\partial t} > 0.01 \\ Y & \text{otherwise} \end{cases} \tag{18}$$

This modification leads to a further increase in the depolarization rate. For $C = 1\ \mu F/cm^2$ and $Y^* \neq Y$ introduced by (18) we obtain: $\dot{V}_{max} = 89.4\ mV/msec$ and $\dot{V}_{max} = 295\ mV/msec$ for $K = 1$ and $K = 4$ respectively. For the same cases, but $Y^* = Y$, we obtain: $\dot{V}_{max} = 74\ mV/msec$ and $\dot{V}_{max} = 269\ mV/msec$.

The duration of AP in the modified VC-D model can be changed without affecting the depolarization phase of AP. It is possible to achieve this by changing the constant $\bar{T}$ in (7), or the function $i_1(V)$, or the angle of inclination of the third linear component of this function. The combination of these options permits us to attain a desired APD while retaining the required shape of AP.

In order to acquire the given APD restitution properties in the VC-D model, we employed the method presented in [11]. According to that approach we represent the time constant $\bar{T}$ in (7) as

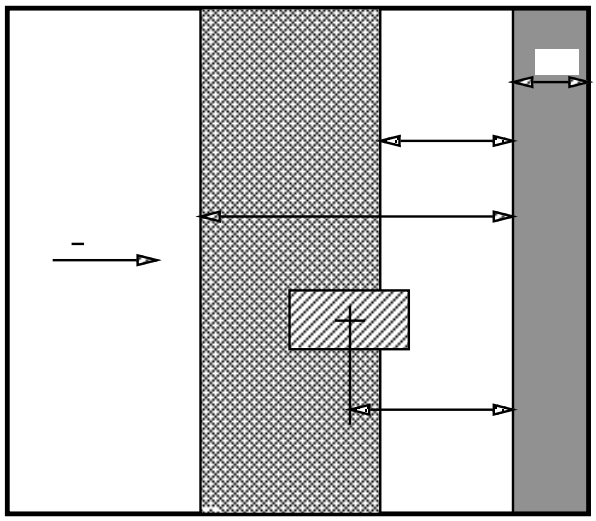

FIG. 6. The geometry of the window of vulnerability for the rectilinear stimulation in isotropic tissue. Θ - direction of the wave propagation, $D1$ - distance between the end of the refractory zone of the first wave and the border of the simulated area, $D2$ - distance between the end of the refractory zone and the nearest edge of the window of vulnerability, $D3$ - distance between the end of the refractory zone and the distant edge of the window of vulnerability, D_s - distance between the end of the refractory zone and the center of the premature stimulated area. Window dimensions: $D1 = 0.96\ cm$, $D2 = -0.04\ cm$ (window of vulnerability overlaps the refractory zone by $0.04\ cm$), $D3 = 0.28\ cm$.

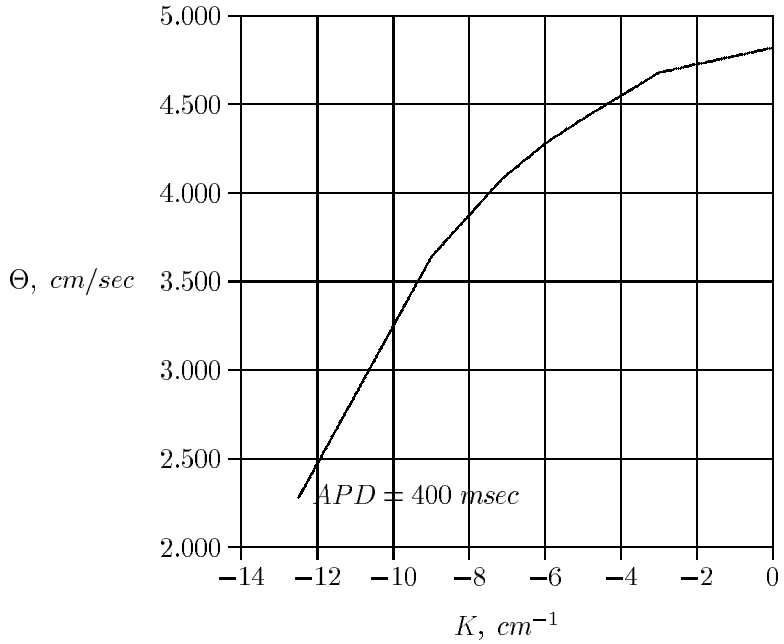

FIG. 5. The dependence of the wave front velocity on the curvature for the original VC-D model.

SUMMARY

These results show that the original VC-D model has the following properties:

- the intensity of depolarization processes is very small and dependent on the growth of the variable Y during the time of depolarization;
- the alternance in AP duration in the case of periodic excitation can hardly be observed (see Fig. 4);
- the amplitudes of the APs produced by the repeatable excitation are decreased and this fact once more confirms the affect of the variable Y during the depolarization phase of AP;
- the asymmetry in time of the depolarization and repolarization phases of AP is well recognized;
- only one of the three conditions required of the simplified model (Karma [24]) is realized in the VC-D model;
- the VC-D model with the original parameters does not lead to nonstationary spiral waves in response to a premature beat.

$0.035 \div 0.057$ cm. Using a grid of 40×40 nodes, the stimulated area becomes (1.4×1.4) cm^2 or (2.28×2.28) cm^2. This size of the simulated area is too small to allow one to neglect the effect of borders on single- and especially multi-spiral wave propagation.

CHARACTERISTICS OF WAVE PROPAGATION

The velocity of rectilinear front propagation in the longitudinal direction is $(\Theta_0)_L = 4.8$ cm/sec for the parameters specified above. In the transverse direction, when $A = 0.25$, $(\Theta_0)_T = 2.4$ cm/sec. The experimental data obtained on a square sheet of canine perecardium [23] give the value of the velocity in longitudinal direction $(\Theta_0)_L = 34$ cm/sec and in the transverse direction $(\Theta_0)_T = 19$ cm/sec. So, the VC-D model predicts velocity of the rectilinear front propagation approximately 10 times smaller than in reality. The dependence of the wave front velocity on the curvature is shown in Fig. 5 . It was obtained by the method proposed in [12] using simulations of wave propagation through narrow pathways with inexcitable parallel borders. One can observe that for $APD = 400$ $msec$ there is a critical curvature $K_{cr} = -12.5$ cm^{-1} and corresponding critical velocity $\Theta_{cr} = 2.3$ cm/sec which is different from zero. Further increase of curvature makes the propagation unstable, and velocity drops to zero.

SPIRAL WAVE FORMATION BY APPLICATION OF PREMATURE BEAT

The premature beat is applied on the tail of the preceding rectilinear wave. There exists a window of vulnerability in space such that the application of a premature stimulus (of area 10×15 nodes, amplitude -40 $\mu A/cm^2$ and duration 10 $msec$) inside this window leads to the appearance of a spiral wave. The geometry of the window of vulnerability in space is shown on Fig. 6 for isotropic tissue.

When a stimulus is applied inside the window of vulnerability the resulting spiral waves are stationary. They rotate around a circle (or ellipse in case of anisotropic tissue) with a constant period $T = 433$ $msec$. The APD of the propagated AP is slightly decreased to 287 $msec$. The variation of APD and coupling resistance does not lead to nonstationary propagation. Premature stimulus application outside the window of vulnerability does not cause a spiral wave but produces a circular response which soon passes out of the simulated area.

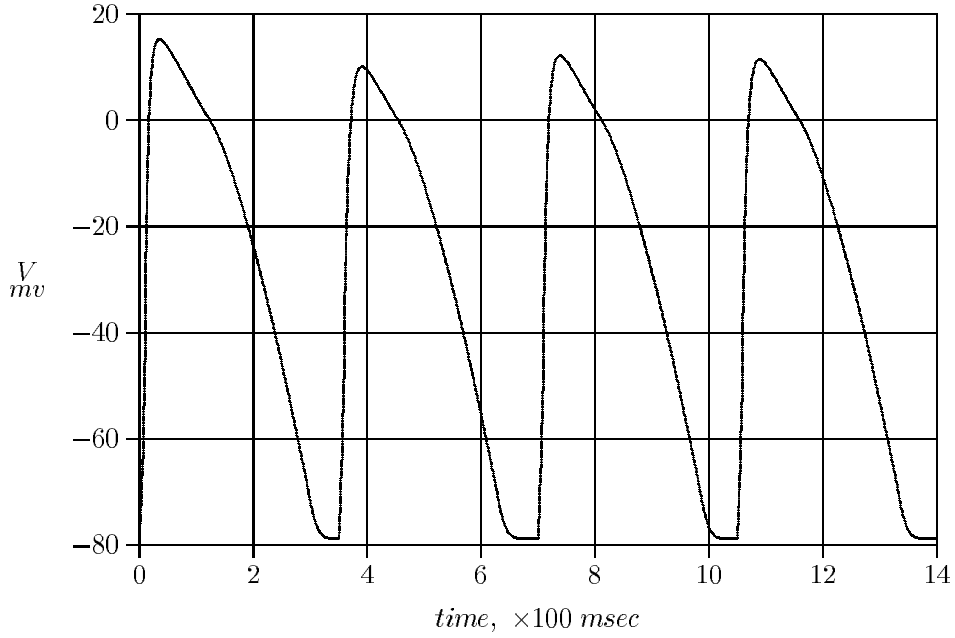

FIG. 4. The action potentials produced by the repeatable excitation for the original VC-D model. Period of excitation 350 *msec*.

DETERMINATION OF THE GRID SPACING

It is well known that for continuous representation of heart muscle tissue

$$i_n = \alpha_x \frac{\partial^2 V}{\partial x^2} + \alpha_y \frac{\partial^2 V}{\partial y^2} = \alpha_x \left[\frac{\partial^2 V}{\partial x^2} + \frac{\alpha_y}{\alpha_x} \frac{\partial^2 V}{\partial y^2} \right] = \alpha_x \left[\frac{\partial^2 V}{\partial x^2} + A \frac{\partial^2 V}{\partial y^2} \right], \tag{14}$$

where: A - anisotropy ratio, $\alpha_x = r/2R_i$, r - radius of a heart cell $[\mu m]$, R_i - specific resistance of intracellular liquid $[k\Omega \cdot cm]$. After finite difference approximation of the partial derivatives for node (i,j) we obtain

$$i_{n_{i,j}} = \frac{r}{2R_i} \left[\frac{V_{i+1,j} + V_{i-1,j} - 2V_{i,j}}{\Delta x^2} + A \cdot \frac{V_{i,j+1} + V_{i,j-1} - 2V_{i,j}}{\Delta y^2} \right], \tag{15}$$

in equations (5) and (15) the left sides are equal, so right sides must also be equal. Therefore

$$r_h = \frac{\Delta x^2}{\alpha_x}; \Delta x = \sqrt{\alpha_x r_h} \tag{16}$$

$$r_v = \frac{\Delta y^2}{\alpha_y}; \Delta y = \sqrt{A \alpha_x r_v} \tag{17}$$

According to [8] $r_h = r_v = 1\ k\Omega \cdot cm^2$ when $A = 1$. So, $\Delta x = \Delta y = \sqrt{r_h \alpha_x}$. For a heart muscle [22] $r = 5 \div 10\ \mu m, R_i = 0.15 \div 0.20\ k\Omega \cdot cm$. Then $\alpha_x = 0.00125 \div 0.00333\ k\Omega^{-1}$ and $\Delta x = \Delta y =$

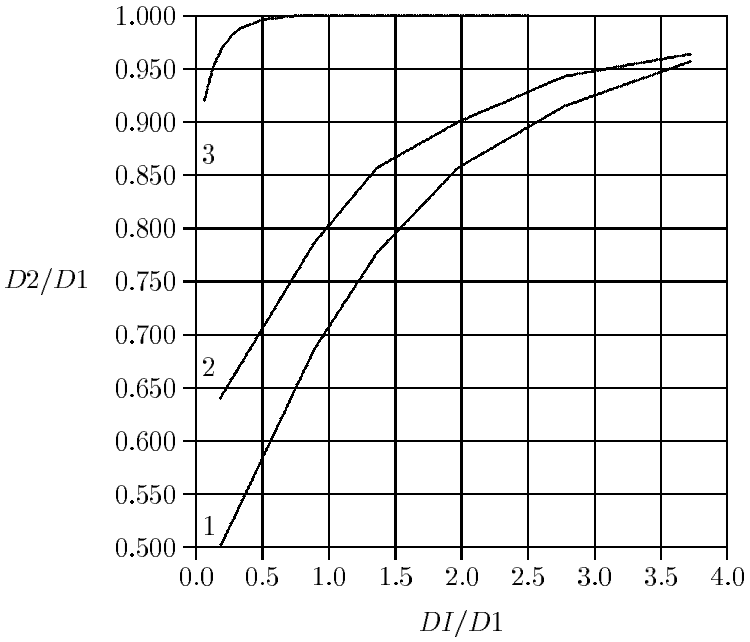

FIG. 3. The restitution curves in normalized form obtained for the normal heart (1), ischemic heart (2) and for the original VC-D model (3).

The obtained value for the depolarization rate is about 50 times smaller than for the normal heart muscle cell [3]. The same ratio is retained for the value of the relaxation parameter.

The AP duration restitution curves are shown on Fig. 3 in normalized form [11]:

$$\frac{D_2}{D_1} = f(\frac{DI}{D_1}), \tag{13}$$

where D_1 - duration of action potential when diastolic interval is infinity, D_2 - duration of AP when diastolic interval is fixed to be equal DI. In Fig. 3 the APD restitution curves are shown for normal and ischemic heart [21], and for VC-D model. The comparison shows significant differences. The cell recovery processes inherent the VC-D model are comparatively short and that explains almost full absence of the APD alteration in the case when repeatable excitation is applied to VC-D model (see Fig. 4).

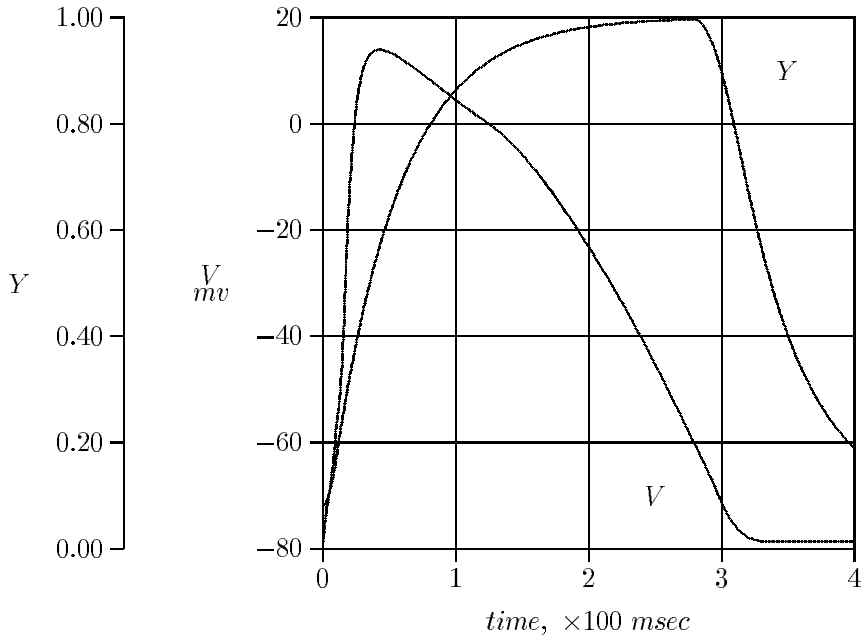

FIG. 1. The AP and gate variable Y as functions of time.

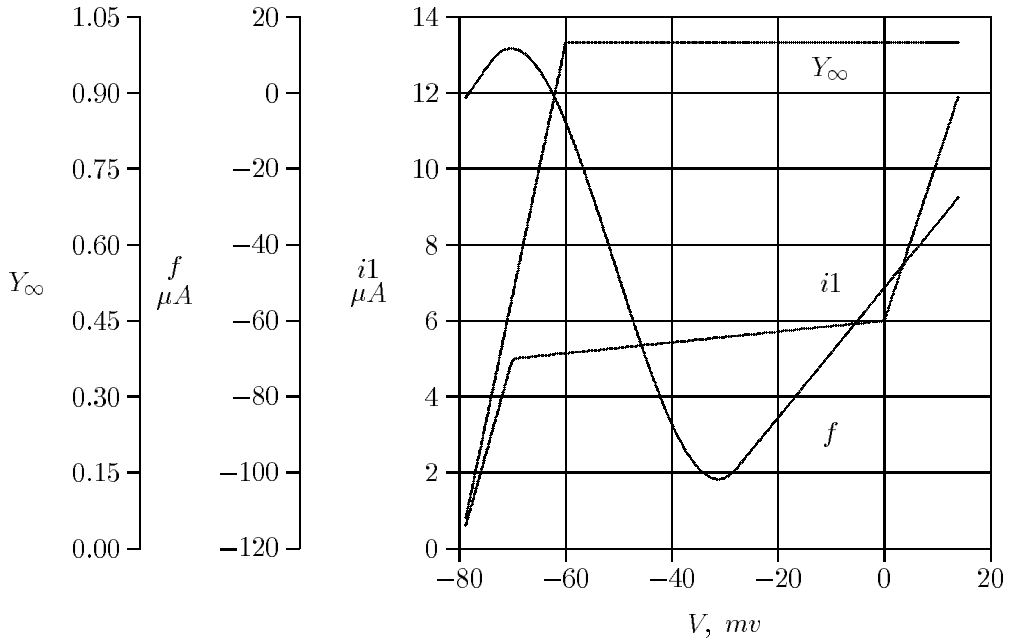

FIG. 2. Functions $Y_\infty(V)$, $f(V)$ and $i_1(V)$.

$$\bar{C} = \frac{C}{100}, \quad \bar{T} = \frac{T}{100} \tag{8}$$

$$f(V) = i_0(V) - i_1(V). \tag{9}$$

The values: $\bar{C} = 0.1$ and $\bar{T} = 0.5$ were used in the original papers [8; 16] and in recent publications [17]. So, $C = 10\ \mu F/cm^2$ and $T = 50\ msec$. The value $C = 10\ \mu F/cm^2$ differs from the experimental values in the literature [20] and with the generally accepted value $C = 1\ \mu F/cm^2$ for the capacity of biological membranes [1; 3]. The continuous functions $i_1(V), f(V)$ and $Y_\infty(V)$ are given in approximated form as:

$$i_1(V) = \begin{cases} 5 + 0.5 \cdot (V + 70) & \text{if } V < -70 \\ 6 + 0.425 \cdot V & \text{if } V > 0 \\ 5 + (V + 70)/70 & \text{otherwise} \end{cases} \tag{10}$$

$$f(V) = \begin{cases} 7.84 + 2 \cdot (V + 74.3) & \text{if } V < -74.3 \\ -98.84 + 1.71 \cdot (V + 27.8) & \text{if } V > -27.8 \\ a \cdot V^3 + b \cdot V^2 + c \cdot V + d & \text{otherwise} \end{cases} \tag{11}$$

$$Y_\infty(V) = \begin{cases} 0 & \text{if } V < -80 \\ 1 & \text{if } V > -60 \\ (V + 80)/20 & \text{otherwise} \end{cases} \tag{12}$$

In $f(V)$ the piece-wise linear approximations are combined with a cubic polynomial. The shape of AP is shown on Fig. 1, and resembles the observed heart muscle AP. It was obtained for the above mentioned data and the following numerical values of cubic polynomial coefficients: $a = 0.003837854, b = 0.584649, c = 25.31834, d = 235.6256$. The initial conditions were: $V(0) = V_{rest} = -78.6$, $Y(0) = 0.0824$. The Runge-Kutta 4 integration method was used with a time step $h = 0.01\ msec$. Functions $Y_\infty(V), f(V)$ and $i_1(V)$ are shown in Fig. 2.

Note that when AP reaches V_{rest} after excitation, the excitability parameter Y gets its maximum value and then continuously decreases with the time constant $\bar{T}$ (Fig. 1). This reflects the recovery processes in the cell after excitation. The main characteristics of AP are:

- Amplitude of AP (90% of the full amplitude of AP) $|V_{max}| = 79,1\ mV$,
- AP duration (measured on the level of 10% of the full amplitude of AP) $APD = 292\ msec$,
- Maximum rate of depolarization $\dot{V}_{max} = 6.8\ mV/msec$,
- Relaxation parameter [10] $\rho = \frac{APD \cdot \dot{V}_{max}}{|V_{max}|} = 25.3$.

these solitary double spiral waves turn into multispiral waves leading to the chaotic excitation of the tissue.

GENERAL DESCRIPTION OF THE VAN CAPELLE AND DURRER MODEL

The model includes two state variables: the transmembrane potential V and a generalized excitability function Y. Y varies between 0 (maximal excitability) and 1 (complete inexcitability). Thus, the single variable Y plays here a role of the m, n and h gate variables in Hodgkin-Huxley kinetics. The behavior of V and Y is expressed by the following system of first order differential equations:

$$C\frac{\partial V}{\partial t} = -Y \cdot i_1(V) - (1-Y) \cdot i_0(V) + i_{ext} \quad (1)$$

$$T\frac{\partial Y}{\partial t} = Y_\infty(V) - Y \quad (2)$$

$$i_{ext} = i_{st} + i_n \quad (3)$$

$$i_n = \nabla(D\nabla V), \quad (4)$$

where: i_{ext} - external current, i_{st} - stimulus current, i_n - total current from neighboring cells, C - membrane capacitance, T - time constant of variable Y, D - diffusion coefficient, $i_0(V)$ - current-voltage relation for fully excitable membrane, $i_1(V)$ - current-voltage relation for fully inexcitable membrane, $Y_\infty(V)$ - steady state excitability function, $\nabla = i\frac{\partial}{\partial x} + j\frac{\partial}{\partial y}$ - gradient operator.

For finite-difference representation of 2D tissue (syncitium), when D is not dependent on x and y

$$i_n = \frac{V_{i+1,j} + V_{i-1,j} - 2V_{i,j}}{r_h} + \frac{V_{i,j+1} + V_{i,j-1} - 2V_{i,j}}{r_v}, \quad (5)$$

where r_h and r_v - coupling resistance between two nodes in the horizontal and vertical directions respectively.

COMPUTER IMPLEMENTATION OF THE ACTION POTENTIAL MODEL

According to [16] the time scale ($\bar{t} = t/100\ msec$) is introduced to the original equations (1), (2) which take the form:

$$\bar{C}\frac{\partial V}{\partial \bar{t}} = -(1-Y) \cdot f(V) - i_1(V) + i_{ext} \quad (6)$$

$$\bar{T}\frac{\partial Y}{\partial \bar{t}} = Y_\infty(V) - Y \quad (7)$$

INTRODUCTION

Modern progress in cell membrane theory and clamp experiment technology led to the development of cardiac cell mathematical models [1; 2; 3] which describe the electrophysiological processes in isolated cells more accurately and in greater detail. These models, while very useful in the reconstruction of Action Potential (AP) of separate cells, cause enormous difficulties in the implementation of computer simulations of AP wave propagation in 2D and 3D cardiac muscles. Even modern supercomputers and massively parallel computer systems can not provide solution times short enough to permit interactive computer simulations. Two approaches are in current use now to avoid these difficulties at least in part: to investigate separately the propagation of wave depolarization fronts [4; 5] and to use simplified models with decreased speed of depolarization [6; 7; 8]. These approaches do not contradict each other but rather illuminate different aspects of the propagation phenomena. Among the simplified models the FitzHugh - Nagumo (FH-N) model is the simplest one. In conjunction with piece-wise approximation of the nonlinear dependencies [9], this model facilitates analytical estimates of the major characteristics of wave propagation and its relation to cell and tissue properties [10]. Many computer simulation studies of 2D and 3D excitable media were performed (see for example [9; 11; 12; 13; 14]) with different modifications of this model. There is some evidence [14; 15] that the FH-N simplified model qualitatively reflects the properties of spiral waves propagation in 2D heart muscle tissue. The FH-N model is not an ionic model in the common sense of the term [15]. The models of Gulko [6] and Van Capelle and Durrer [8] are closer to ionic models and represent more accurately the shape of the action potential. The Van Capelle and Durrer model in comparison with the FH-N model does not require greatly increased computational resources and has therefore become widely used [8; 16; 17; 18; 19]. But the characteristics and parameters of this model even in recent publications remain the same as were introduced by VC-D in 1980. In the original form, this model was intended for implementation on PC and that put some limitations on the parameters of the cell model, spacing between grid nodes, size of the modeling tissue and coupling resistance between the nodes. Now it is possible to eliminate most of these constraints by implementing this model on a massively parallel computer.

The major objective of this study is to illuminate the properties of the original VC-D model and its limitations, to modify this model so to make it closer to reality, to expand the size of the modeled tissue by using the Connection Machine CM-2. On the basis of these modifications we investigate the initiation of nonstationary spiral waves in 2D tissue and one of the possible situations when

Abstract

The properties of the Van Capelle and Durrer (VC-D) simplified model are studied to estimate how adequately they reproduce the physiological properties of cardiac cells and tissue. It is shown that the transition from a membrane capacitance 10 $\mu F/cm^2$, used in previous studies, to 1 $\mu F/cm^2$, the introduction of adjustable action potential duration restitution, and the appropriate adjustment of action potential duration (APD) leads to simulation result closer to the reality. In particular, it is shown that in the 2D model of anisotropic tissue, nonstationary propagation of spiral waves in response to premature beat is possible when the cells of the tissue have specific APD restitution properties. The continuous pacemaker activity in this case leads to the creation of multiple spiral waves.

The Van Capelle and Durrer Model of Cardiac Action Potential Generation and 2D Propagation: Modifications and Application to Spiral Wave Propagation

Part I

B. Y. Kogan, W. J. Karplus, M. G. Karpoukhin
Computer Science Department, University of California, Los Angeles, California

Keywords: Van Capelle and Durrer simplified model, 2D spiral waves, Action Potential Duration Restitution, simulation on parallel computers.